A Bayesian change-point analysis of electromyographic data: detecting muscle activation patterns and associated applications

TIMOTHY D. JOHNSON[†]

Department of Biostatistics, School of Public Health, Univeristy of Michigan, Ann Arbor, MI 48109, USA

tdjtdj@umich.edu

ROBERT M. ELASHOFF

Department of Biomathematics, UCLA School of Medicine, Los Angeles, CA 90095, USA

SUSAN J. HARKEMA

Department of Neurology and The Brain Research Institute, UCLA School of Medicine, Los Angeles, CA 90095, USA

SUMMARY

Many facets of neuromuscular activation patterns and control can be assessed via electromyography and are important for understanding the control of locomotion. After spinal cord injury, muscle activation patterns can affect locomotor recovery. We present a novel application of reversible jump Markov chain Monte Carlo simulation to estimate activation patterns from electromyographic data. We assume the data to be a zero-mean, heteroscedastic process. The variance is explicity modeled using a step function. The number and location of points of discontinuity, or change-points, in the step function, the inter-change-point variances, and the overall mean are jointly modeled along with the mean and variance from baseline data. The number of change-points is considered a nuisance parameter and is integrated out of the posterior distribution. Whereas current methods of detecting activation patterns are deterministic or provide only point estimates, ours provides distributional estimates of muscle activation. These estimates, in turn, are used to estimate physiologically relevant quantities such as muscle coactivity, total integrated energy, and average burst duration and to draw valid statistical inferences about these quantities.

Keywords: B-Splines; Change-point analysis; Electromyography; EMG; Non-constant variance; Reversible jump Markov chain Monte Carlo; Step-function.

1. INTRODUCTION

Muscles and nerves generate electrical activity during muscle activation and the myoelectric signal can be recorded by electromyography (EMG) (Loeb and Gans, 1986). EMG activity recorded from the lower limb muscles is used to assess neuromuscular activity during locomotion. Muscle activation patterns can provide insight into the neural control of locomotion. After neurologic injury, such as a spinal cord

---

[†]To whom correspondence should be addressed

injury (SCI), locomotion recovery is limited and the muscle activation patterns of the lower limbs are significantly altered. For example, coactivity of the muscles of the lower limbs may be significantly altered resulting in impaired gait. Interventions to ameliorate the recovery of locomotion may attempt to do so by improving muscle coactivity. Changes in muscle coactivity during neuro-rehabilitation, as well as the effects of load, speed, and task mechanics on coactivity are areas of active research that would also benefit from a quantifiable measure of coactivity (Neptune *et al.*, 1997). It is our goal in this paper to present a method of quantifying muscle activation patterns and its associated error which are then used to estimate physiologically releveant parameters such as muscle coactivity, average burst duration, and total integrated energy. We adopt a Bayesian approach to this problem.

Many physiological quantities of interest can be defined in terms of the muscle activation patterns as recorded by EMG. In particular, the relevant information we need is in the alternating pattern of neuromuscular activity and inactivity. The first step then is to estimate when a muscle is active and when it is inactive. Several algorithms and computer-based methods have been developed to detect muscle activation patterns from an EMG signal (see, for example, reviews by Hodges and Bui (1996) and Staude and Wolf (1999)). However, none of these provide estimates of the error associated with the activation pattern. These errors are necessary to assess the variation incurred in estimating coactivity as well as other physiological quantities. In this paper we present a new method for muscle activation detection that allows statistically valid inferences to be easily drawn. Our method is based on estimating the heteroscedastic variance in EMG data and computing the signal-to-noise (SNR) ratio with 'large' values indicating neuromuscular activity. We identify changes in the variance of the EMG signal using a Bayesian multiple change-point model with an *a priori* unspecified number of change-points. This allows functions of the posterior distribution to be computed and valid inferences to be drawn. We use reversible jump Markov chain Monte Carlo (RJMCMC) (Green, 1995) simulation to estimate the posterior distribution of model parameters. RJMCMC is a generalization of the Metropolis–Hastings MCMC algorithm that allows the dimension of the parameter space to change, thus allowing moves between models that differ in their number of parameters.

In the next section, we discuss current approaches to detecting onset of muscle activity and their associated shortcomings. We present our model in Section 3 along with the details of the RJMCMC sampler. Applications from EMG data are given in Section 4. We discuss the ramifications of model assumption violation in Section 5 and conclude the paper with a discussion in Section 6.

2. CURRENT METHODOLOGY

Before presenting current methodology, we briefly overview EMG. Muscles have the special property that they can convert electrical energy into mechanical work. Neurons and muscle fibers are connected in a one to many relationship. Each muscle fiber is innervated by only one neuron; however, one neuron innervates tens to thousands of muscle fibers. A motor unit comprises a single neuron and the muscle fibers it innervates. For example, it is estimated that there are 610 motor units in the tibialis anterior (TA) with 445 fibers per motor unit for a total of 271 450 TA muscle fibers (Perry, 1992). When a neuron fires it sends an action potential down its axon to the muscle fibers that it innervates. This action potential causes a release of a neurotransmitter across the interface of the terminal end of the axon and the muscle cell membrane which generates an action potential over the cell membrane surface. Action potentials are an all or none phenomenon. If the input is greater than a threshold, the action potential fires and is always of a specific magnitude. The magnitude of the action potential is determined by the physical properties of the neurons and muscle fibers. Larger neurons and muscles fibers generate larger action potentials than do their smaller counterparts. EMG records these action potentials. The EMG bipolar electrode that measures this energy is taped to the surface of the skin over the muscle of interest. The resulting EMG signal is a

complex interference pattern of thousands of action potentials that vary in magnitude—there are different muscle fiber types in each muscle; in time—different motor units may be firing asynchronously and at differing rates; and in space—the distance between the electrode and each muscle fiber is different and the fibers a single neuron innervates are dispersed heterogeneously throughout the muscle. A detailed account of muscle physiology can be found in Berne and Levy (1993). Details of EMG and what it is measuring can be found in Loeb and Gans (1986).

Many physiological quantities of interest in assessing EMG data (see Section 4) can be defined as functions of the muscle activation patterns as measured through the EMG signal. Two methods are currently used to determine onset and cessation of muscle activity. An experienced physiologist visually determines them or one uses a computer based method. The first method is subjective and highly dependent on the experience and biases of the experimenter. In an attempt to remove these deficiencies, computer based methods have been proposed (Hodges and Bui, 1996) that detect changes in muscle activity. The most commonly used methods perform the following steps (Hodges and Bui, 1996): first, the EMG signal is high-pass filtered to remove low-frequency signals caused by passive movement of the electrodes and cables due to muscle contraction and floor impact (Perry, 1992). This results in a symmetric, zero mean process. Second, the data are *full wave rectified* by taking the absolute value of the data. Third, the rectified data are band-pass filtered (this smoothed estimate of the mean of the rectified data is called the linear envelope). Fourth, a local mean of the resultant data is calculated at each time point. Onset of muscle activity is established when the SNR—defined here as the ratio of the full-wave rectified and smoothed signal mean to the full-wave rectified and smoothed baseline mean—first becomes greater than some multiple of the baseline standard deviation. Once a muscle is active, a drop in the SNR to less than some multiple of the baseline standard deviation constitutes cessation of muscle activity. Band-pass filtering removes high-frequency noise components on a global scale. Statistical models that use global smoothing to estimate the mean hitherto assume that the error terms have constant variance (Eubank, 1988). However, a glimpse at the residual plot (not shown) reveals that the rectified data do not have constant variance. Hence, this assumption is violated and significantly complicates assessment of the error. Finally, the bandwidths used to smooth the data are not optimally chosen—they are selected by what appears reasonable for the data at hand (Hodges and Bui, 1996) or by using a single global kernel in all situations instead of using a more objective method such as cross-validation (Eubank, 1988). In principle, one could attempt to remove these deficiencies by approximating the model error, defining a test statistic, and endeavoring to determine the asymptotic distribution of the test statistic (note in this connection EMG patterns from several consecutive steps are analysed as one single time series. EMG patterns from consecutive steps are correlated and so steps are not analysed as independent observations, which makes it difficult to assess the standard error by bootstrap methodology). Instead, we adopt a Bayesian approach that is well suited for this problem and circumvents this arduous task.

3. THE MODEL

In a general setting, consider a non-stationary time series $Y = (Y_i)_{i=1}^{N}$ whose first two moments depend on time according to the following model:

$$Y_t = \mu(t, \theta) + f^{1/2}(t, \phi)\varepsilon_t. \tag{1}$$

Here μ is the mean function dependent on time and perhaps a parameter set θ, ε_t are independent, zero mean, constant variance 1 error terms, and f is a strictly positive function of time and possibly the parameter set ϕ. The intersection of θ and ϕ need not be null. Variants of this type of heteroscedastic model have been extensively used in finance theory and econometrics since the early 1980s when Engle (1982) introduced the autoregressive conditional heteroscedasticity (ARCH) model which was subsequently

generalized (GARCH) by Bollerslev (1986). These models were developed to model the volatility present in several different economic phenomena and have appeared numerous times in one form or another in the finance and econometrics literature (see the reference list in Bollerslev *et al.* (1992)). Specifically, ARCH models the conditional variance as a function of past sample variances while leaving the unconditional variance constant. GARCH allows the conditional variance to further depend on lagged conditional variances. The linear GARCH(p,q) model thus specifies the function f in (1) as

$$f(t) = \alpha_0 + \sum_{i=1}^{q} \alpha_i (y_{t-i} - \mu(t-1))^2 + \sum_{j=1}^{p} \beta_i f(t-1)$$

where the parameter sets θ and ϕ are implied with ϕ equal to the p lagged conditional variances and the q lagged sample variances. Positivity constraints must also be imposed on the α and β. When $p = 0$ this model is the ARCH model and when $p = q = 0$ the model reduces to white noise. These models are useful in predicting the daily volatility of stock market indices.

Prediction of a new value is not our aim and we therefore allow f to be an arbitrary, strictly positive function. A general, nonparametric estimate of f can be obtained by splines (de Boor, 1978; Wahba, 1990). In this paper, we handle the positivity constraint by modeling $\log(f)$ and estimate it with a first-order spline (i.e. by a step function). We also assume that the data are a zero mean process and reflect this in our prior for $\mu(t, \theta)$.

Let the EMG signal be denoted by $Y = (Y_i)_{i=1}^{N}$ with observed value y measured at times t_i. In our particular application, the time points are equally spaced, $\delta \equiv t_{i+1} - t_i = 1$ millisecond for all i and there are no missing data. Further we assume that $t_1 = 0$ and $t_N = T$. Suppose there are k change-points. The location of the jth change-point will be denoted by $c_j \in (0, T)$. Let $c_0 \equiv 0$ and $c_{k+1} = T$. Define $c^{(k)} = (c_i)_{i=1}^{k}$. The interval between the jth and $(j + 1)$th change-points will be denoted by I_j. That is, $I_j = [c_j, c_{j+1})$ for $j = 0, \ldots, k - 1$ and $I_k = [c_k, c_{k+1}]$. Within I_j let $f = \sigma_j^2$. Hence, within interval I_j, $Y_i \sim N(\mu, \sigma_j^2)$ where μ is the overall mean of the EMG data. The vector of baseline EMG data will be denoted by $Z = (Z_i)_{i=1}^{M}$ with observed value z. We further assume that the ε_i are iid $N(0, 1)$. The baseline data are modeled iid $N(\mu_b, \sigma_b^2)$. Different muscles are modeled separately. We emphasize here that the baseline signal is collected when the leg is at rest before the beginning of the experiment and is a distinct and separate time series from the EMG signal. The EMG and baseline data from a single muscle are jointly modeled.

$\mathcal{M}_k$ will denote the model with k change-points. Conditional on $c^{(k)}$, we have a $(k + 4)$-dimensional parameter space: the mean and variance of the baseline, the mean of the EMG signal and variances for each of the $k + 1$ intervals I_j. Let $\sigma^{2(k)} = (\sigma_i^2)_{i=1}^{k}$. We gather these parameters into the two vectors $\theta^{(k)} = (\mu, \sigma^{2(k)}, c^{(k)})$ and $\theta^{(b)} = (\mu_b, \sigma_b^2)$. We consider the hierarchical structure for the joint distribution of $(k, \theta^{(k)}, y)$:

$$p(k, \theta^{(k)}, y) = p(k)p(\theta^{(k)} \mid k)p(y \mid k, \theta^{(k)}).$$

The baseline data are assumed independent of the EMG data so the full joint posterior is

$$p(k, \theta^{(k)}, \theta^{(b)}, y, z) = p(k)p(\theta^{(b)})p(\theta^{(k)} \mid k)p(y \mid k, \theta^{(k)})p(z \mid \theta^{(b)}).$$

3.1 *Prior distributions and Likelihood*

For model selection, that is the number of change-points, we assume a uniform distribution on the integers $0, \ldots, L$ where L is a predetermined maximum. Conditional on $\mathcal{M}_k$, the change-point locations $c^{(k)}$ are

distributed as the even-numbered order statistics from $2k + 1$ points iid $U(0, T)$ (Green, 1995). Hence, the prior distribution of the change-point locations is

$$p(c_1, \ldots, c_k) = (2k + 1)! \, T^{-2k} c_1 (c_2 - c_1) \cdots (c_k - c_{k-1})(1 - c_k/T).$$

Further, $\mu \sim N(0, 1)$ and $\xi_j \equiv \ln(\sigma_j^2) \sim N(7.5, 100)$ for $j = 0, \ldots, k$. For the baseline data, $\mu_b \sim N(0, 1)$ and $\sigma_b^2 \sim$ Inv-gamma$(0.001, 0.001)$ all independently of one another. The $N(0, 1)$ prior for the mean of the EMG signal reflects our belief that the overall mean is zero. The log variances of the EMG signal range from approximately 3.5 to 11.5. The $N(7.5, 100)$ prior for the log variance was chosen by centering it over this range and scaling it to be rather flat over 3.5 to 11.5. The priors for the baseline mean and variance are standard conjugate priors for normal data. The parameters for these priors reflect our belief that the baseline has a mean of zero. However, we do not know, *a priori*, the variance and so choose a vague prior for it.

We assume that within I_j the data are iid $N(\mu, \sigma_j^2)$. Let n_j denote the number of observed points in the time series in interval I_j. The log likelihood, given model k and ignoring the baseline data, is

$$-\frac{1}{2} \sum_{j=1}^{k+1} \left[n_j \ln(2\pi\sigma_j^2) + \frac{1}{\sigma_j^2} \sum_{y \in I_j} (y - \mu)^2 \right].$$

The log likelihood of the baseline is

$$-\frac{1}{2} \left[n \ln(2\pi\sigma_b^2) + \frac{1}{\sigma_b^2} \sum_{j=1}^{n} (z_j - \mu_b)^2 \right]$$

where n is the number of points in the baseline data.

3.2 *Possible transitions*

We systematically propose updates to the parameter. However, one could also consider randomly updating model parameters. At each iteration, we propose an addition of a change-point and then propose a deletion. Next, we propose location updates followed by proposals for the EMG data mean and then for the inter change-point variances. Finally, we update the baseline mean and variance by sampling directly from their joint posterior. If the current model is $\mathcal{M}_L$, we do not propose a change-point addition; likewise, if the current model is $\mathcal{M}_0$, a deletion and change of location are not possible and these steps are ignored.

The location for a new change-point is proposed at random on the interval $(0, T)$. This location must lie within an existing interval I_j with probability 1. To preserve identifiability, this new change-point is labeled c_{j+1} with the indices of all subsequent change-points being incremented by 1. Given model $\mathcal{M}_k$, a deletion is proposed by selecting a change-point randomly and uniformly on the integers $1, \ldots, k$.

3.3 *Dimension-matching*

By adding or deleting change-points, we respectively increase or decrease the dimension of the parameter space. Thus, when proposing a jump between subspaces, dimension-matching criteria must be defined between the two subspaces to insure that these moves are well defined and so that detailed balance is achieved (Green, 1995).

In model $\mathcal{M}_k$ to propose a new change-point, c^*, within interval $I_j = [c_j, c_{j+1})$ we define dimension-matching between the current log variance, ξ_j, and the proposed new log variances ξ_j', ξ_{j+1}' defined on

$[c_j, c^*)$ and $[c^*, c_{j+1})$, respectively. We assume that the current log variance is well supported in the posterior and so we draw $x \mid \xi_j \sim N(\xi_j, 0.5)$ and then make the transformation

$$\xi'_{j+1} = x$$
$$(c_{j+1} - c_j)\xi_j = (c^* - c_j)\xi'_j + (c_{j+1} - c^*)\xi'_{j+1}.$$

The second equation above separates the new log variances as a weighted average of the current log variance with weights equal to the lengths of the intervals on which they are defined. The 0.5 variance was chosen empirically to give a reasonable rate of convergence and good mixing properties. A change-point deletion at c_j is proposed by taking the weighted average of the two current log variances ξ_{j-1} and ξ_j defined on $[c_{j-1}, c_j)$ and $[c_j, c_{j+1})$. Hence the new log variance ξ^*_{j-1} is related to ξ_{j-1} and ξ_j by

$$(c_{j+1} - c_{j-1})\xi^*_{j-1} = (c_{j+1} - c_j)\xi_j + (c_j - c_{j-1})\xi_{j-1}.$$

3.4 *Proposal density ratios*

Proposing changes to a mean, variance or change-point is straightforward following the Metropolis–Hastings algorithm (Metropolis *et al.*, 1953; Hastings, 1970). Specifically, we propose a new mean by drawing from $N(\mu, \zeta^2)$. A new log variance, ξ'_j, for the jth interval is proposed by drawing from $N(\xi_j, \nu^2)$. A change to the location, c_j, of the jth change-point is proposed by drawing from a truncated $N(c_j, \min(c_{j+1} - c_j, c_j - c_{j-1})/\lambda)$ with support (c_{j-1}, c_{j+1}). ζ^2, ν^2, and λ are adjusted during the first 5000 iterations so that the acceptance rates are in the range of 25% to 35%.

For proposals that move across subspaces, the form of the acceptance probability is more complicated and may be written as (Green, 1995)

$$\min[1, (\text{l.r.}) \times (\text{proposal ratio}) \times (\text{prior ratio}) \times (\text{Jacobian})] \tag{2}$$

where l.r. stands for likelihood ratio. To insure detailed balance, the density ratio of the random variates drawn for dimension matching purposes and the Jacobian of the dimension matching transformation must be included in the density ratio.

In particular, the proposal density ratio for a change-point addition at c^* in I_j is

$$(\text{l.r.}) \times \frac{T}{k+1} \times \frac{(2(k+1)+1)! \, (c^* - c_j)(c_{j+1} - c^*)}{(2k+1)! \, (c_{j+1} - c_j) \, T^2} \tag{3}$$

$$\times \frac{1}{\sqrt{200\pi}} \exp\left[-\frac{1}{200}\left\{(\xi'_j - 7.5)^2 + (\xi'_{j+1} - 7.5)^2 - (\xi_j - 7.5)^2\right\}\right] \tag{4}$$

$$\times \sqrt{\pi} \exp\left[(x - \xi_j)^2\right] \times \frac{c_{j+1} - c_j}{c_{j+1} - c^*}. \tag{5}$$

The last two terms in (3) are the proposal ratio for this particular move type and the prior ratio for the number and location of change-points, respectively. The term in (4) is the prior ratio for the log variances. The first term in (5) is the the reciprocal of the conditional density of the random variate x drawn for dimension matching purposes and the last term is the Jacobian of the dimension matching transformation. The proposal density ratio for a deletion of an existing change-point is the reciprocal of this expression.

4. Applications

We now apply our model to the analysis of EMG data. First, we apply our method to EMG data during locomotion from a non-disabled subject and from a SCI subject. The estimated activation patterns are used

to define coactivity. We compare coactivity patterns from the SCI subject at two different speeds and show that coactivity changes with speed in the SCI subject. Second, we estimate the total area under the linear envelope. Third, we apply our model to muscle activity from an individual with a spinal cord injury during forced dorsi-flexion (physically flexing the foot toward the knee). Our primary interest is in three major muscles of the lower leg—the MG, the Soleus, and the TA. The Soleus and MG are plantar flexors and the TA is a dorsi flexor.

The data are recorded and digitized at 1000 Hz. A high-pass zonal filter (Pratt, 1991), with a cutoff frequency of 40 Hz, is applied to remove low-frequency signals that are a result of passive movement of the electrodes and cables due to mechanical movement and floor impact (Perry, 1992). The resulting signal is zero-mean and non-stationary (Staude and Wolf, 1999). Within I_j we assume that the signal is iid $N(\mu, \sigma_j^2)$.

Post simulation processing of the results from the RJMCMC sampler to detect patterns of muscle activity and inactivity forms the basis of our applications. We use the posterior distribution of the variance within each interval I_j and the variance of the baseline to detect these patterns. Specifically, we use the SNR defined as the square-root of the ratio of the signal variance to that of the baseline (Mauger and Brown, 1995). The baseline noise is obtained by recording 1 s of EMG while the muscles are at rest prior to applying the experimental condition. Mathematically, the SNR in interval I_j is

$$\text{SNR}_j = \sqrt{\sigma_j^2 / \sigma_b^2}.$$

We define the muscle as active in I_j if $\text{SNR}_j \geqslant 2.5$ and inactive otherwise. Further, any duration of activity less than 30 ms is considered to be a noise spike and any duration of inactivity less than 39 ms is considered to be an artifact of the interference pattern which may occur when the net sum of all the action potentials reaching the bipolar electrode cancel each other out (Beres *et al.*, 2002). Noise spikes are removed and interference artifacts, typically occuring during rather long period of activity, are 'turned on' and included as part of the activity burst.

Our focus is on detecting the activation patterns in the EMG signal and not on model selection. Hence, we treat the number of change-points as nuisance parameters and integrate them out of the estimated posterior distribution. We ran each simulation for 50 000 iterations discarding the first 20,000 iterations as a burn-in. We reduce the inherent autocorrelation in the chain by saving every tenth iteration. Hence, we estimate the posterior distribution with 3,000 samples from the Markov chain. The maximum allowable number of change-points was 500—more than twice as many as needed for all datasets analysed.

Convergence of model parameters in a reversible jump algorithm is difficult to assess because the definition of model parameters may change across subspaces. Brooks and Giudici (1998) suggest monitoring convergence on any set of model parameters whose definition does not change across subspaces. Coactivity, area, and average burst duration (all defined subsequently) are the parameters of interest and do not change definition across models. Hence, we monitor convergence on these parameters. Each chain was run three times. The largest estimated potential scale reduction (Gelman and Rubin, 1992), $\hat{R}$, was less than 1.05.

4.1 *Coactivity during locomotion*

In this section we use our methodology to compare coactivity in an individual with a spinal cord injury at two different speeds. EMG data from six consecutive steps on a treadmill at 1.8 mph from the SCI subject (8.578 s) and 1.2 mph (10.465 s) and from a representative non-disabled subject at 1.8 mph (8.087 s) were recorded and analysed. The six steps were analysed as a single, long time series and not as six separate data sets. CPU times for these data sets are given in Table 1.

Table 1. *CPU times for the RJMCMC method. Code written in C and run on a PC with a 700 MHz AMD Athalon processor. For comparison, the conventional method took less than a minute for each subject/muscle combination*

Muscle	CPU Time in Minutes		
	SCI, 1.2 mph	SCI, 1.8 mph	Non-disabled
Sol	97.8	86.8	38.7
MG	83.3	80.7	49.2
TA	72.2	53.9	46.6

Changes in coactivity across speeds is an important factor for locomotor training interventions. We define coactivity between two muscles as half the sum of the proportion of time two muscles are simultaneously active to the total time either muscle is active and the proportion of time two muscles are simultaneously inactive to the total time either muscle is inactive. A value of one indicates perfect coactivity; a value of zero indicates no coactivity. Partition the intervals for muscle $i = 1, 2$ into those where there is activity, $\mathcal{A}_i$, and those without activity, $\mathcal{A}'_i$. Further, subscript interval j for muscle i by I_{ij} and let m denote Lebesgue measure. Then coactivity between muscles 1 and 2 is

$$COA(1, 2) = 0.5 \left\{ \frac{\sum_{I_{1j} \in \mathcal{A}_1} \sum_{I_{2j} \in \mathcal{A}_2} m(I_{1j} \cap I_{2k})}{m(\cup_{i=1}^{2} \cup_{I_{ij} \in \mathcal{A}_i} I_{ij})} + \frac{\sum_{I_{1j} \in \mathcal{A}'_1} \sum_{I_{2j} \in \mathcal{A}'_2} m(I_{1j} \cap I_{2k})}{m(\cup_{i=1}^{2} \cup_{I_{ij} \in \mathcal{A}'_i} I_{ij})} \right\}. \quad (6)$$

The first summand above gives a measure of how often the two muscles are simultaneously active relative the total time either muscle is active; the second summand is a measure of the relative simultaneous inactivity. Note that many of the intersections in the numerators above will be empty. In the unlikely event that the two muscles are always active, the second summand above is ignored. Similarly if both muscles are always inactive, we ignore the first summand above.

Figures 1 and 2 show the EMG data and the estimated SNRs from a randomly selected step from the non-disabled subject and from the SCI subject (1.8 mph), respectively. Muscle activation patterns are easily detected from the SNR plots. Histograms of the number of change-points are displayed in Figure 3. The maximum allowable number of change-points was 500—well above the range observed. Posterior density estimates of coactivity for the non-disabled subject and the SCI subject are displayed in Figure 4. Coactivity means and standard deviations are tabulated in Table 2 along with their differences. The coactivities between the TA and either the Soleus or MG are larger in the SCI subject than in this representative non-disabled subject. We can compute the posterior probability that the coactivity in the SCI subject stepping at 1.8 mph is greater than that at 1.2 mph by determining the percentage of differences that lie above zero. These posterior probabilities are given in the last column of Table 2. These probabilities suggest that speed affects coactivity in this individual.

4.2   *Total area under the linear envelope*

A quantity that is commonly quoted in EMG analysis is the total area under the linear envelope. The linear envelope is an estimate of the mean of the rectified EMG signal. Given our model, the expected value of the absolute value of the EMG signal, the rectified signal, is a constant times the standard deviation. In particular if $y \sim N(0, \sigma^2)$, then $E(|y|) = \sqrt{2\sigma^2/\pi}$. The EMG data from the first step from the non-disabled subject was rectified and smoothed with a smoothing spline (the function *smooth.spline* in S-PLUS) with the smoothing parameter selected by cross-validation. The areas for the three muscles are tabulated in Table 3. The estimated areas under the rectified and smoothed curves are given in the first
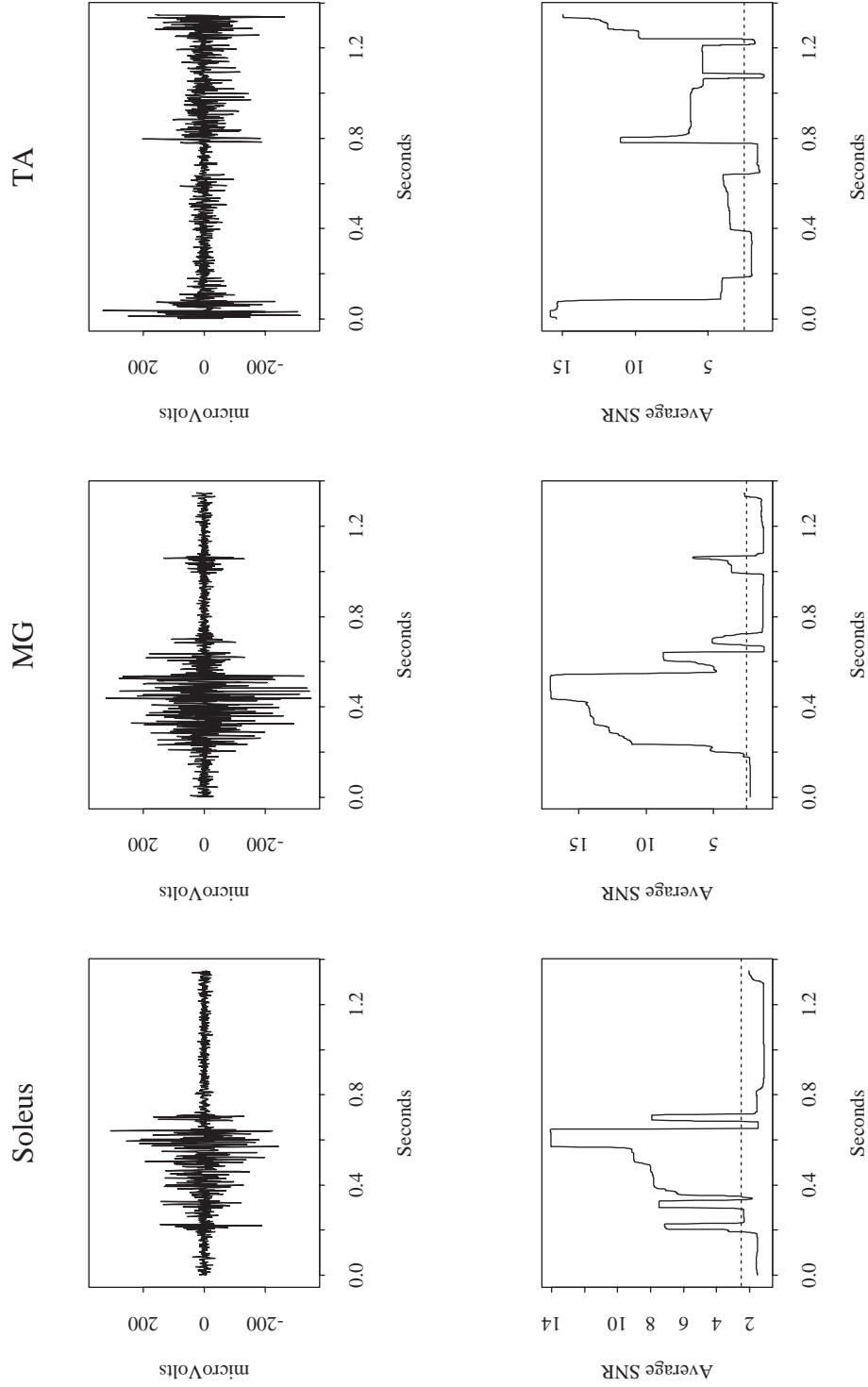
Fig. 1. EMG trace from a non-disabled subject during stepping (one step) for the Soleus, MG and TA muscles (top panels) with their corresponding estimated average SNR (bottom panels). The horizontal dashed line is the SNR threshold of 3. Analyses performed on all steps as one long time series.
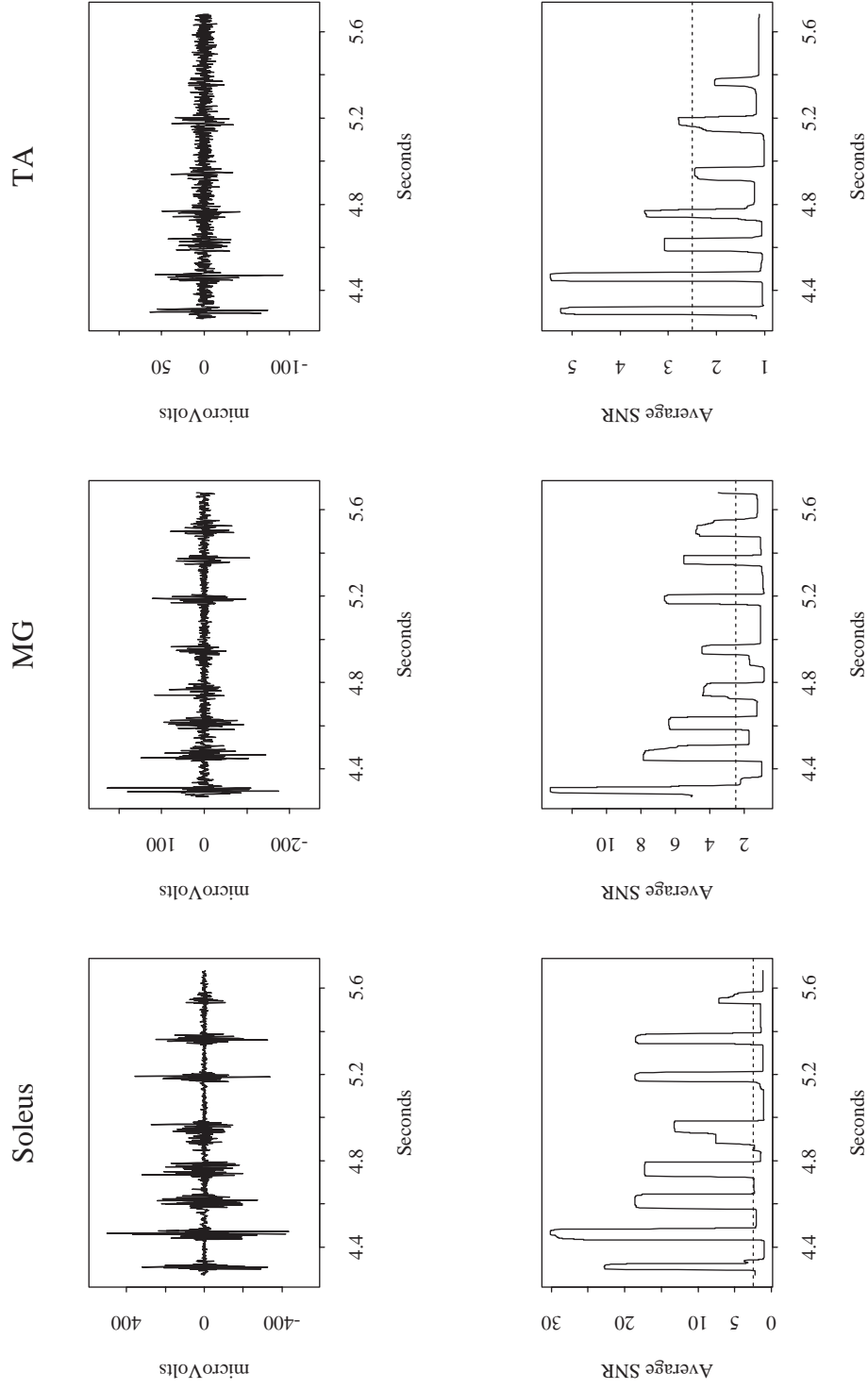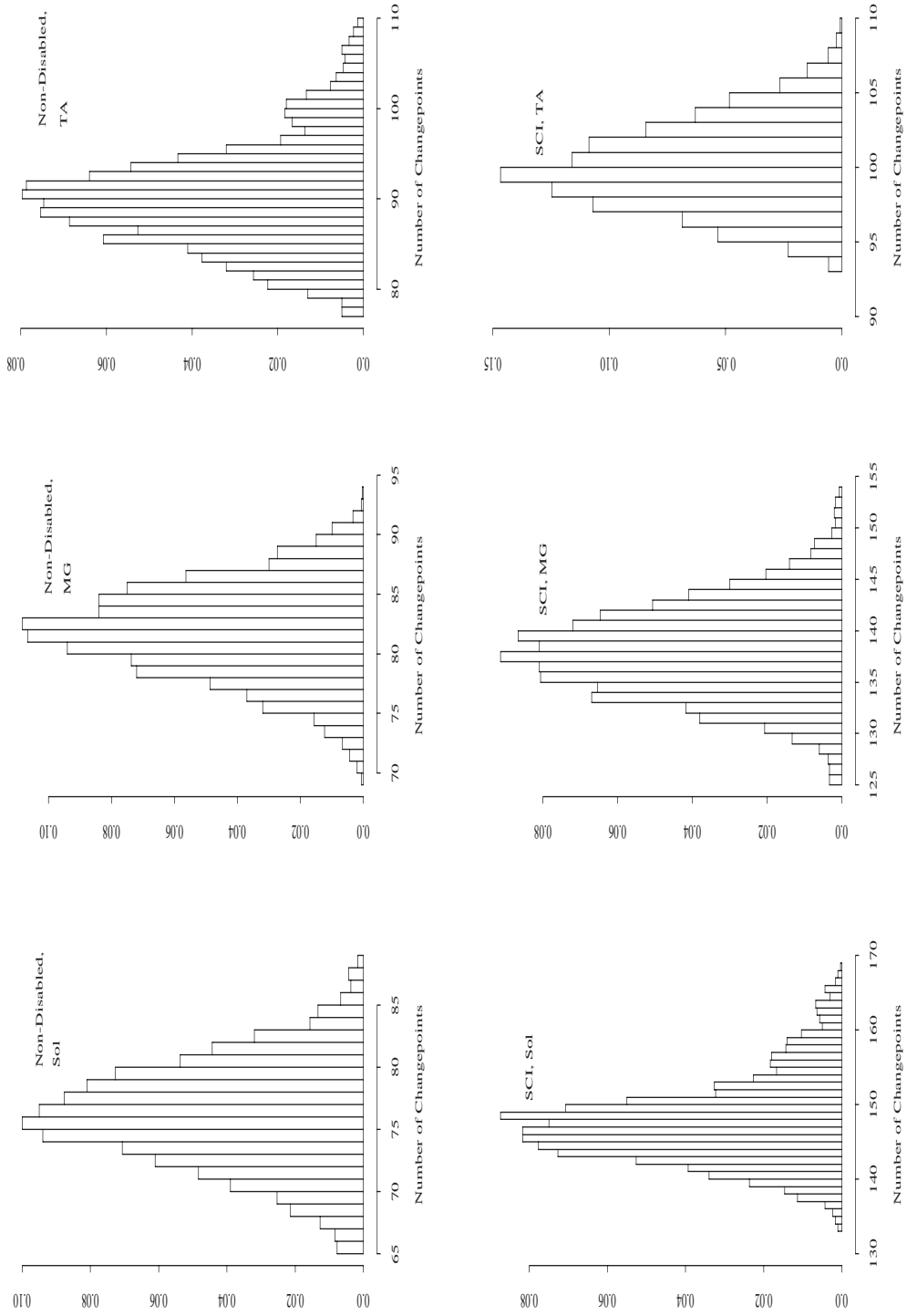
Fig. 2. EMG trace from a SCI subject during stepping at 1.8 mph (one step) for the Soleus, MG and TA muscles (top panels) and their corresponding estimated average SNR (bottom panels). The horizontal dashed line is the SNR threshold of 3. Analyses performed on all steps as one long time series.

Fig. 3. Histograms of the number of changepoints. Top row—non-disabled subject; bottom row—SCI subject stepping at 1.8 mph. Maximum allowable number of changepoints—500.
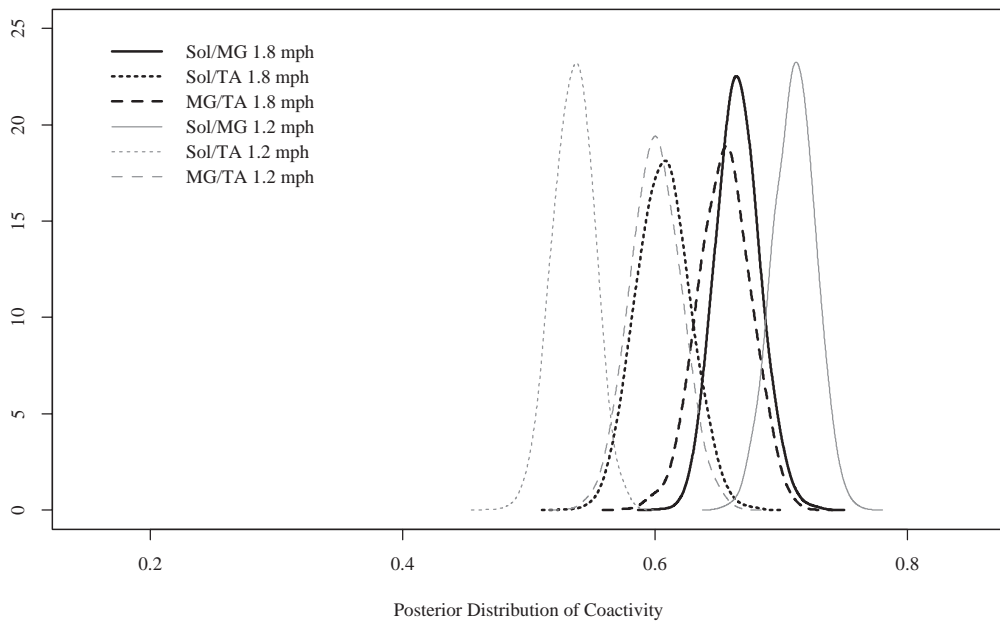
Non-disabled Subject
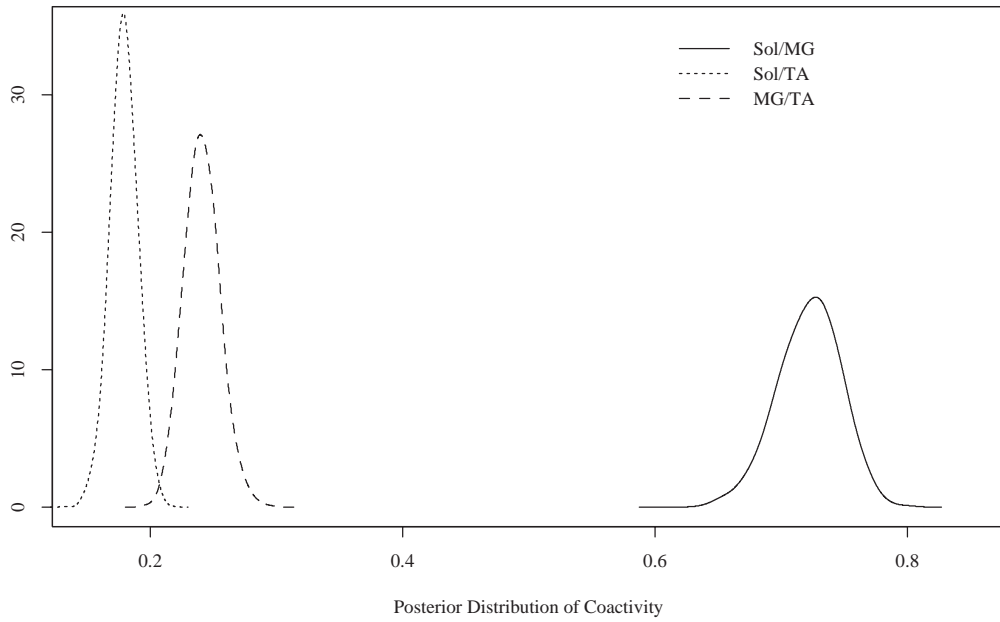
SCI Subject

Fig. 4. Posterior density estimates of coactivity between the lower leg muscles in a non-disabled subject (upper panel) and a SCI subject (lower panel).

Table 2. *Coactivity means and standard deviations between the Soleus and the TA, the Soleus and the MG, and the MG and the TA. The last column is the posterior probability that the coactivity measured for the SCI subject at 1.8 mph is greater than at 1.2 mph*

	SCI, 1.2 mph		SCI, 1.8 mph		Difference		
Coactivity	Mean	S.D	Mean	S.D.	Mean	S.D.	$Pr(COA_{1.8} > COA_{1.2})$
Sol. and MG	0.710	0.017	0.666	0.017	-0.044	0.024	0.037
Sol. and TA	0.535	0.016	0.607	0.021	0.071	0.027	0.997
MG and TA	0.601	0.020	0.655	0.021	0.055	0.029	0.966
	Non-disabled						
Sol. and MG	0.722	0.025					
Sol. and TA	0.179	0.011					
MG and TA	0.241	0.014					

Table 3. *Area under the linear envelope estimates in µV-sec*

Muscle	Rectified	RJMCMC	0.025 quantile	0.975 quantile
Sol	29.58	28.27	26.79	29.88
MG	40.99	40.50	38.37	42.93
TA	39.69	38.63	36.69	40.75

column. The estimated area from our model is given in the second column. The last two columns give the lower and upper 0.025 quantiles from our model. The estimated area obtained by rectifying and smoothing the data are well supported under the estimated posterior distribution of the total area.

4.3 *Average burst duration during passive dorsi-flexion*

We recorded 2 s of EMG from the Soleus, MG, and TA during passive dorsi-flexion—the foot is passively moved toward the knee by a therapist. This is a clinical test to measure the level of spasticity that commonly occurs after spinal cord injury (Ashby and McCrea, 1987). Figure 5 shows EMG traces for this dataset along with their estimated mean SNRs (the rapidly changing muscle activity pattern seen here is called *clonus*). The estimated SNRs of the three muscles are shown superimposed on one another in Figure 6. It is evident from this figure that the activity patterns of the three muscles are synchronized.

The average (activity) burst duration, average inter-burst duration, and frequency of bursts are important factors for understanding the underlying physiology of clonicity after spinal cord injury. Although we can compute the posterior distribution of the inter-burst duration and burst frequency, we only focus on the average burst duration. The average burst duration for muscle i is defined as

$$\sum_{I_{ij} \in \mathcal{A}_i} m(I_{ij}) \Big/ N_i$$

where N_i is the number of bursts. That is, sum up the total time of activity and divide by the number of distinct periods of activity. The posterior densities of the average burst duration for the Soleus, MG, and TA are displayed in Figure 7 and their means and standard deviations are reported in Table 4.

The Soleus average burst duration is substantially longer than that of the MG which is substantially longer than that of the TA. In general, the Soleus is activated earlier than the MG and becomes inactive later than the MG. Likewise, the MG is typically activated early than the TA and becomes inactive later (see Figure 6).
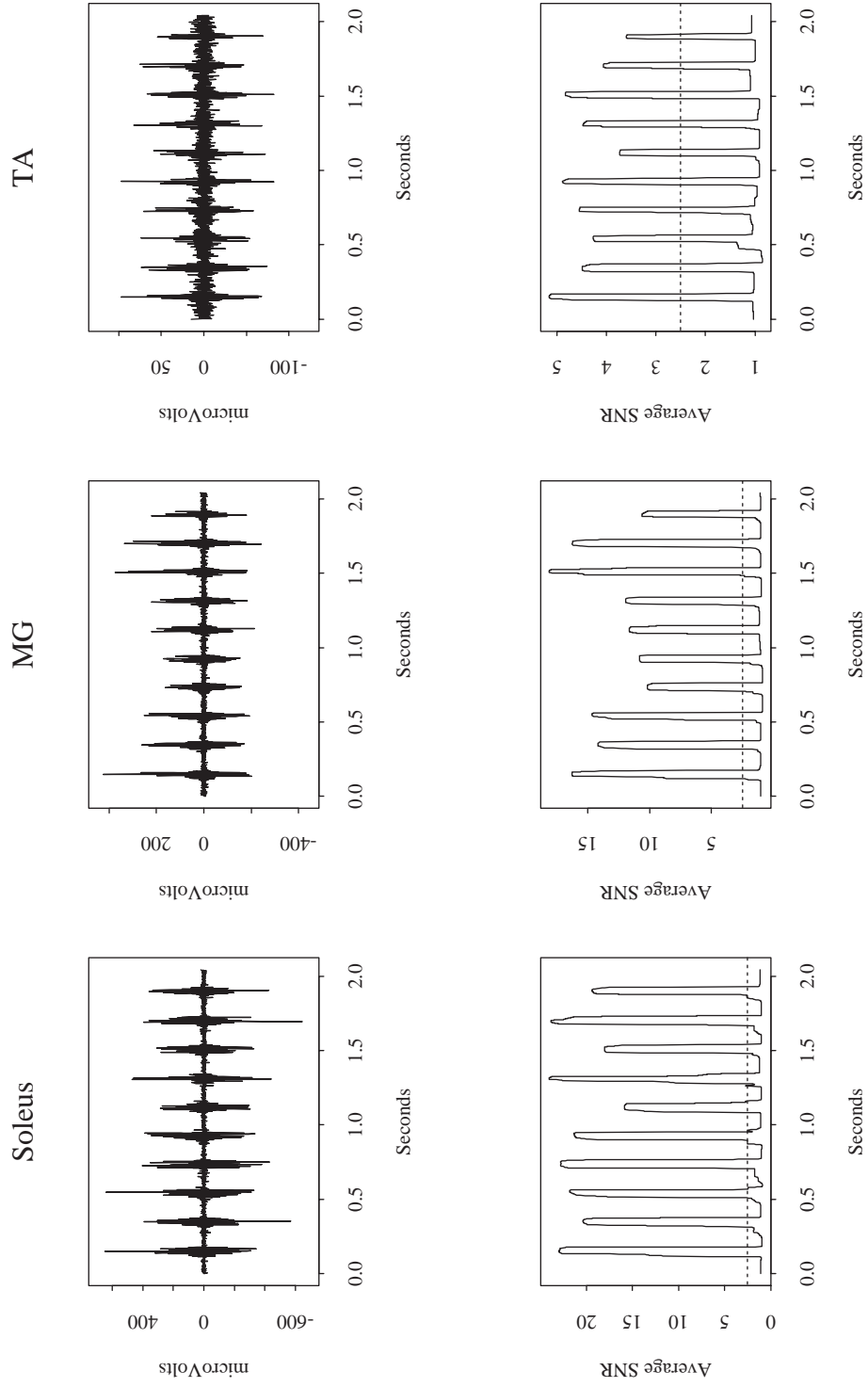
Fig. 5. EMG traces during passive dorsi-flexion of the Soleus, MG and TA muscles from a SCI subject and their corresponding estimated average SNR (bottom panels). The horizontal dashed line is the SNR threshold of 3.
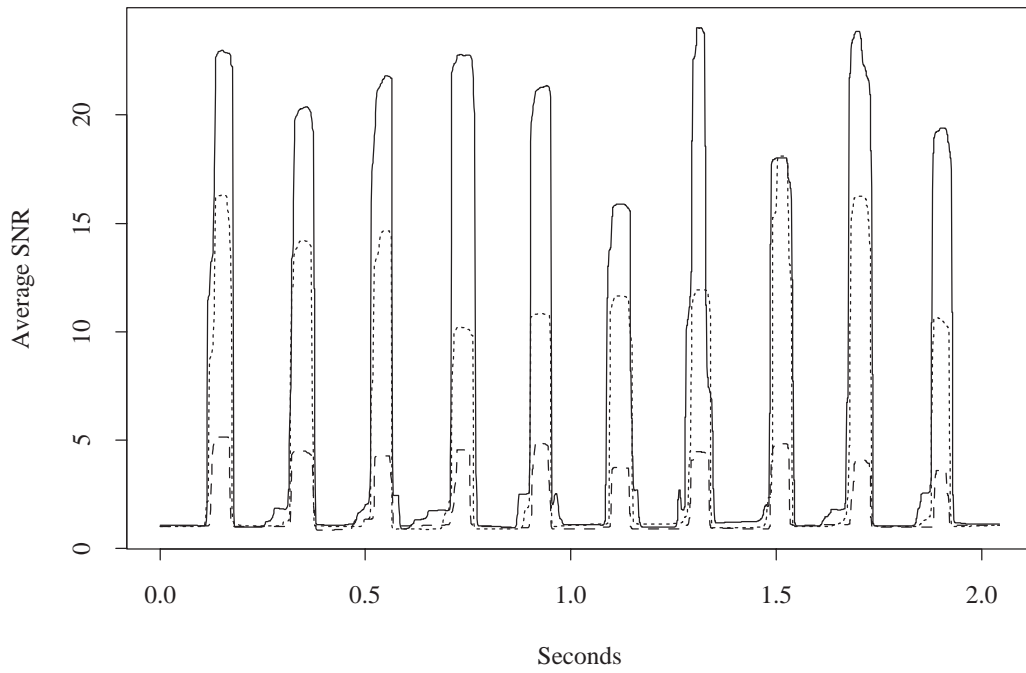
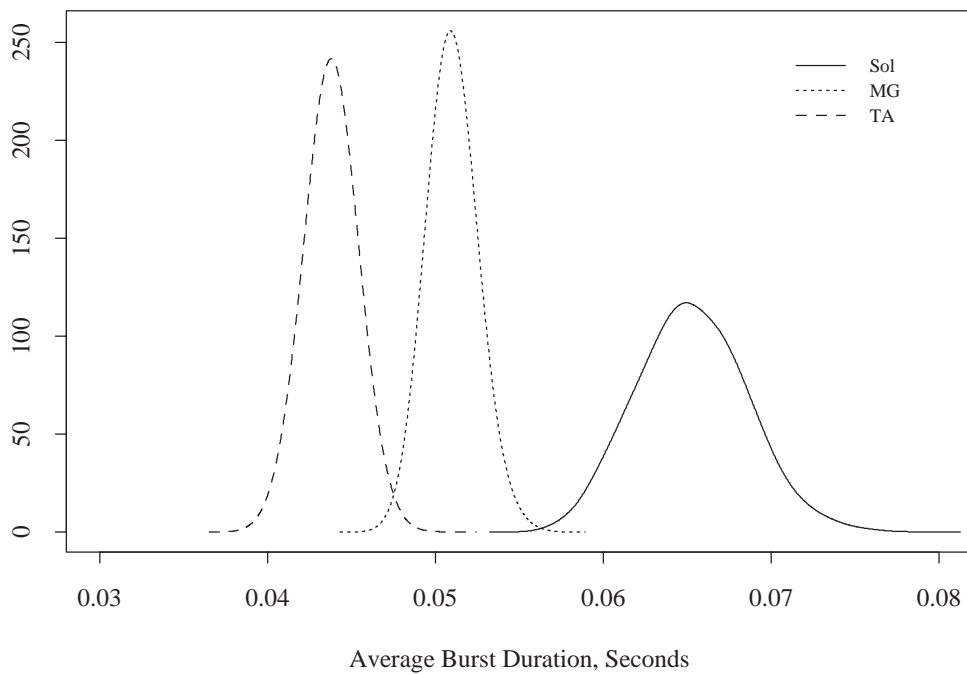Fig. 6.   Signal-to-noise ratio during passive dorsi-flexion. Soleus —, MG · · · , TA - - -.

Fig. 7.   Posterior density estimates of average burst duration of the lower leg muscles during passive dorsi-flexion in a SCI subject.

Table 4. *Average burst duration means and standard deviations during passive dorsi-flexion*

Muscle	Mean (sec.)	S.D.
Soleus	0.0628	0.0033
MG	0.0510	0.0012
TA	0.0438	0.0013

5. ROBUSTNESS AGAINST VIOLATION OF MODEL ASSUMPTIONS

For our model, we assume that the data are iid $N(\mu, \sigma_j^2)$ within I_j, and that the baseline data are iid $N(\mu_b, \sigma_b^2)$. A spectral analysis of the passive dorsi-flexion data suggests that this assumption is violated. Figure 8 shows several power spectra from the SCI subject. The first column of panels show the power spectra of the baseline Soleus and MG signals. There is a strong frequency component at 160 Hz that accounts for approximately 35% of the variability in the Soleus baseline signal and about 25% of the variability in the MG baseline signal. There are several smaller frequency components in each signal— each account for less than 4% of the variability in the data. We also observed frequency components in the EMG signal between change-points. In the inactive regions, the same frequency component is present in both the Soleus and the MG (second column of panels). The power spectra of the Soleus and MG, during a period of muscle activity, are displayed in the third column of panels. When the Soleus is active we observed a second, stronger frequency component at approximately 110 Hz. These two components account for approximately 33% (at 110 Hz) and 27% (at 160 Hz) of the variability observed during Soleus activity. In the MG, the only dominant frequency component occurs at 110 Hz accounting for approximately 55% of the total variability. Similar frequency components are also present in the TA. The spectral contents of EMG signals are comprised of many complex and poorly understood factors (Loeb and Gans, 1986) and thus we do not speculate on the physiological relevance and meaning of these frequency components. Nevertheless, the question arises whether our model is robust against this violation.

To answer this question, we simulated two clonic-like activity patterns to mimic the Soleus and the MG, along with baseline data. We wish to know whether our estimates of coactivity and average burst duration are robust against this model assumption violation. We consider the following model:

$$y_t = A\cos(2\pi f_1 t + \phi_1) + B\cos(2\pi f_2 t + \phi_2) + \varepsilon_t.$$

Here, ε_t are iid $N(0, \sigma^2)$ random variables, f_1 and f_2 are the signal frequencies, A and B are the component amplitudes, and ϕ_1 and ϕ_2 are the phases.

One second of data sampled at 1000 Hz, every 0.001 s, with $f_1 = 0.16$, $A = 1.0$, $B = 0$, and $\phi_1 = 0$ was generated to simulate the baseline frequency component. Noise was added by choosing σ^2 so that 35% of the total variability of the Soleus, and 25% of the total variability of the MG, is due to the 160 Hz frequency component.

We simulated fifty clonic-like activity patterns of the Soleus and MG by alternately simulating periods of inactivity with periods of activity. For the Soleus, we simulated 11 periods of inactivity with $A = 1.0$, $B = 0$, and $f_1 = 0.16$. We added noise by selecting σ^2 so that 35% of the total variability is due to the 160 Hz frequency component. Since phase shifts and offsets at the interface between periods of activity and inactivity may affect the location of the change-points, we randomly selected the phase, ϕ_1, for each of these inactivity periods from the set

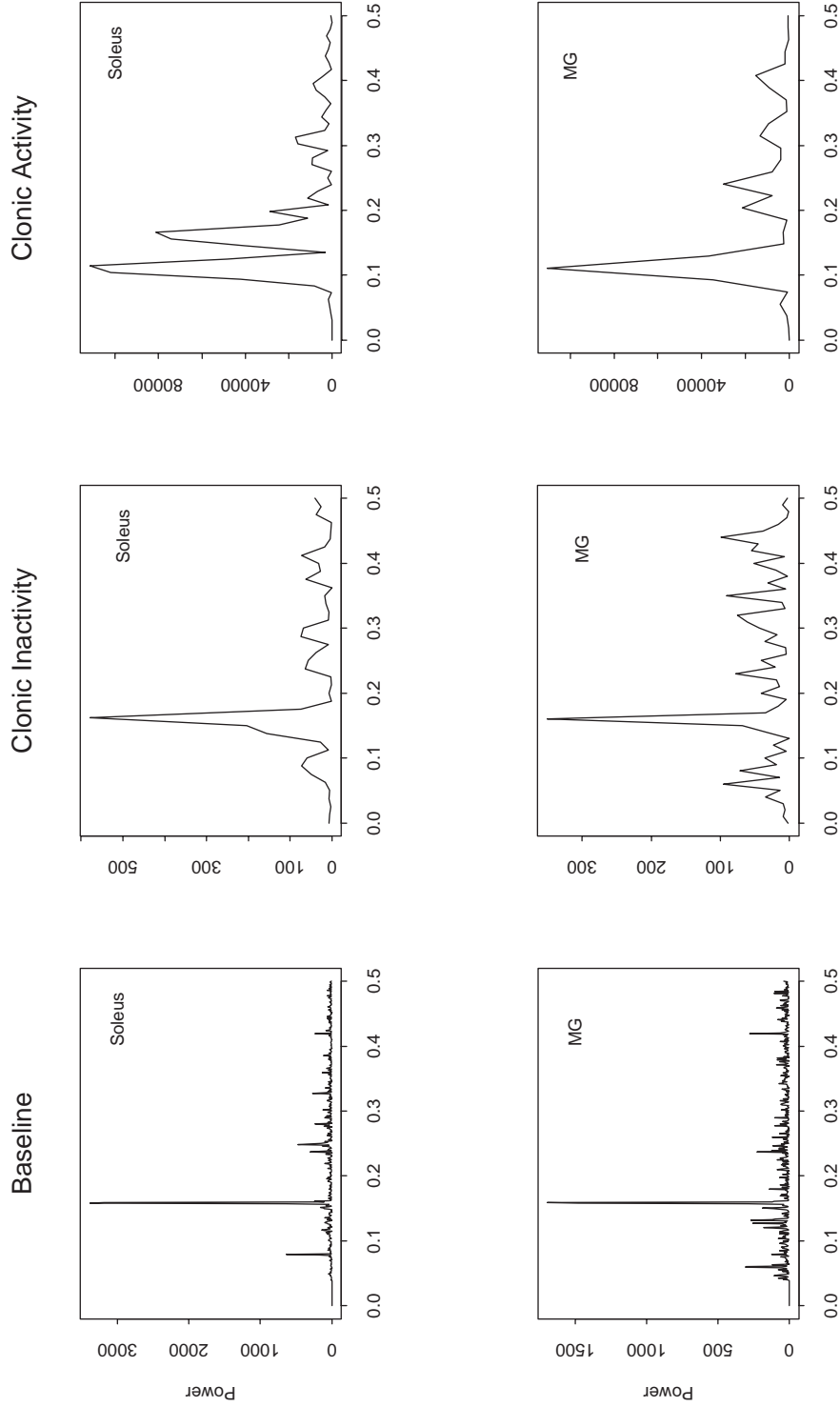$$\{-3\pi/4, -\pi/2, -\pi/3, -\pi/4, 0, \pi/4, \pi/2, 2\pi/3, 3\pi/4, \pi\}.$$

Fig. 8. Power spectra from the baseline and EMG signals of the Soleus and the MG from the SCI subject. The last two columns of figures are spectra from a single period of inactivity and activity during forced dorsi-flexion.
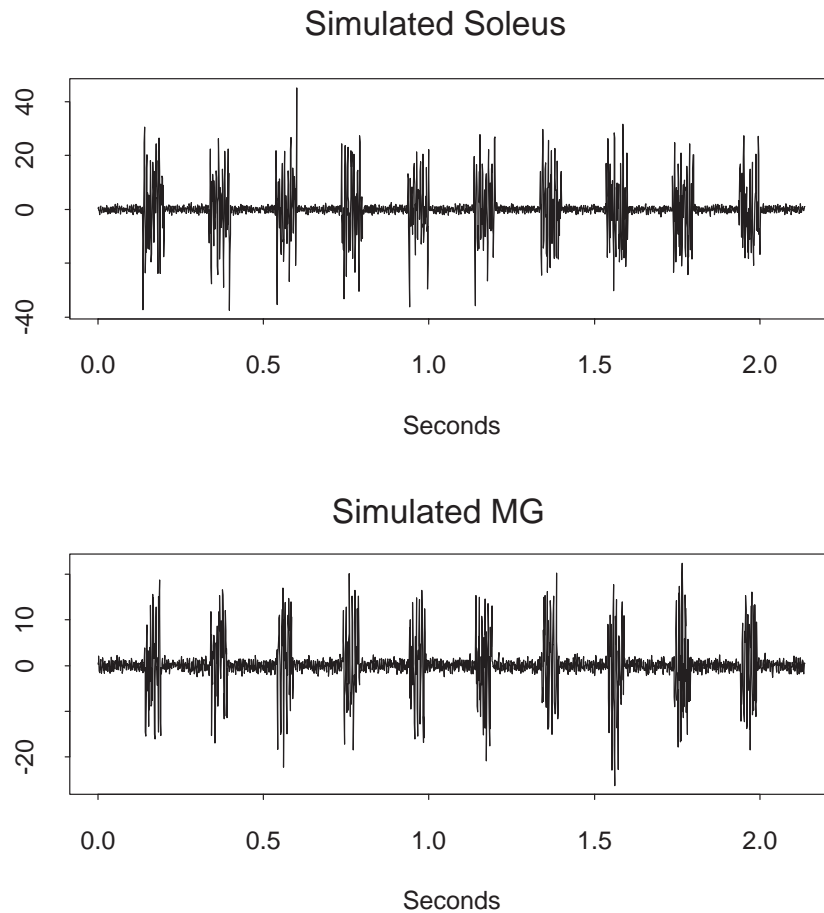
Simulated Soleus

Seconds

Simulated MG

Seconds

Fig. 9. Examples of our simulated Soleus and MG clonic-like activity patterns.

To simulate the 10 periods of activity, we set $A = B = 10$, $f_1 = 0.11$, $f_2 = 0.16$, and randomly selected ϕ_1 and ϕ_2 from the set of phases above. The length of each period of activity (in miliseconds) was drawn from $N(65, 5)$ (so the average burst duration is $N(65, 0.5)$. The lengths of the inactive periods were drawn from $N(135, 5)$. For the MG, we also simulated 11 periods of inactivity alternating with ten periods of activity. For the inactivity periods, $A = 1.0$, $B = 0$, and $f_1 = 0.16$. We added noise so that 25% of the total variability is due to the frequency component. We randomly selected the phase, f_1, for each inactivity period from the set above. We simulated the ten activity periods by setting $A = 10$, $B = 0$, and $f_1 = 0.11$. Each phase was selected from the above set of phase angles. Each period of inactivity was drawn from $N(150, 5)$ except the first and last which were set to 140 ms and 145 ms long, and each period of activity was drawn from $N(50, 5)$. Figure 9 shows one simulated pair of data.

Figures 10, 11 and 12 display the results of the simulation. Each histogram is based on pooling the results from the 50 simulations. The true average burst durations are 65 ms and 50 ms, respectively for the simulated Soleus and MG. Our pooled estimates (means) of the posterior mean average burst duration are 64.8 ms and 50.2 ms, respectively. The variance of the average burst durations was 0.5 ms for both the simulated Soleus and MG. Our pooled estimates (medians) were 0.6 ms for the Soleus and 0.7 ms
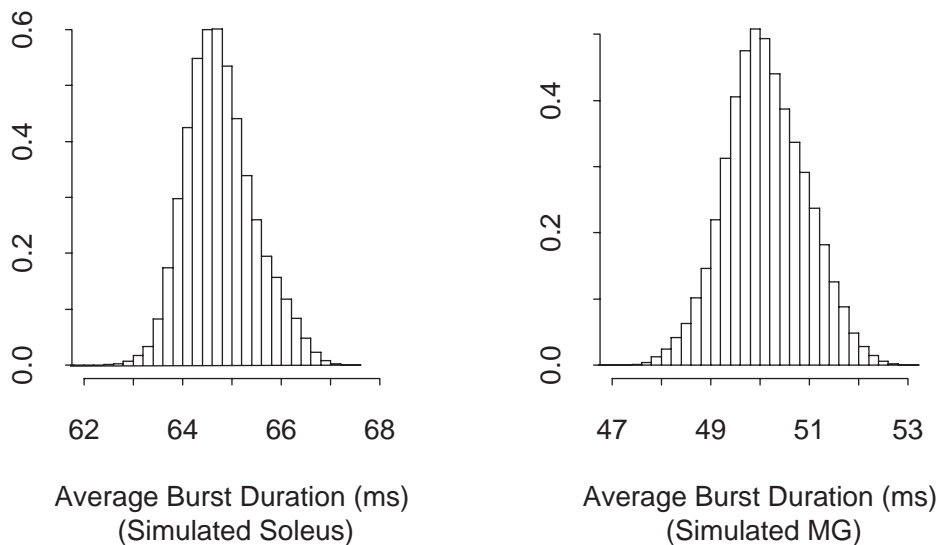
Fig. 10. Estimated posterior distribution of ABD from our simulated Soleus and MG data pooled over all ten simulations. True Soleus ABD = 65 ms. True MG ABD = 50 ms.
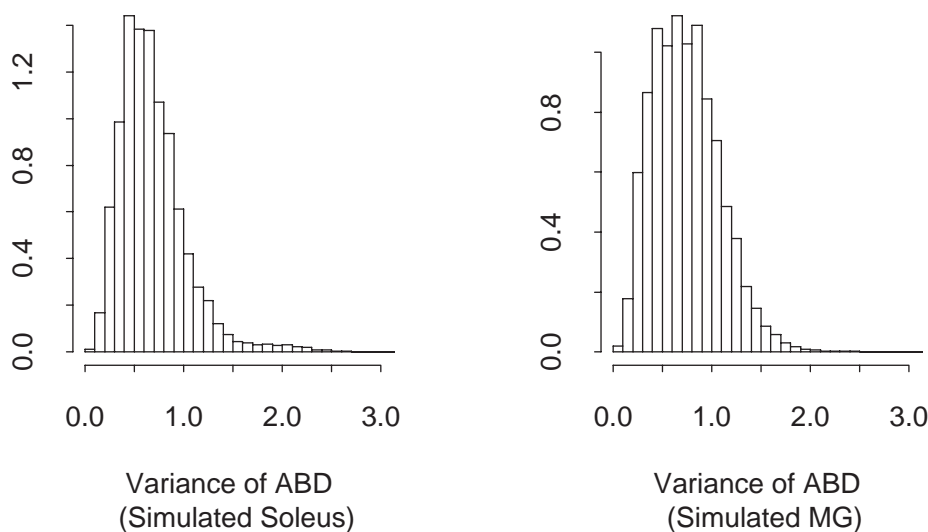

Fig. 11. Estimated posterior distribution of the variance of the ABD from our simulated Soleus and MG data pooled over all ten simulations. True Soleus Var of ABD = 0.5. True MG Var of ABD = 0.5.

for the MG. The mean coactivity between the two simulated EMG patterns is 0.839. The estimate of the posterior (pooled) mean coactivity is 0.842. For comparison, we also ran the current methodology Hodges and Bui (1996) on the simulated data. The current methodology, for determining onset and cessation of muscle activity during walking, band-pass filters the rectified data (50–1000Hz) followed by taking local averages (window width = 25). When the local average is greater than three times the baseline average for more than 50 consecutive points, the muscle is said to be active, when it drops below three times the
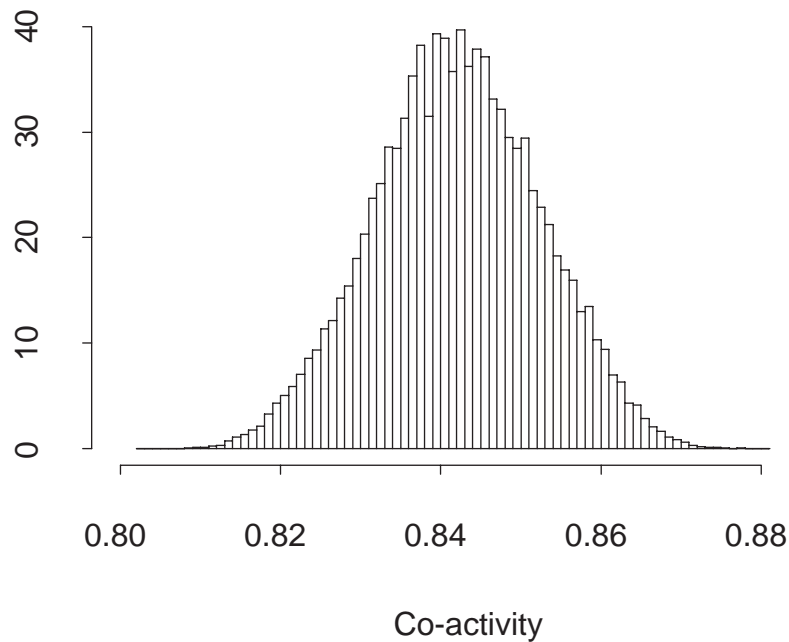
Fig. 12. Estimated posterior distribution of coactivity from our simulation based on pooling our ten simulations. True coactivity = 0.839.

baseline average for more than 150 consecutive points, the muscle is said to be inactive. For our simulated data, these numbers did not suffice and we had to 'tune' the values to get reasonable results. Our window width for the local averages was 5 for the Soleus and 10 for the MG. A muscle became active if it was above three times baseline average for more than 25 consecutive points and became inactive if it was below three times baseline average for more than 75 consecutive points. The average coactivity was 0.835 (s.e. 0.05). The average burst duration for the Soleus was 65.9 ms (s.e. 2.2) and the average burst duration for the MG was 50.0 ms (s.e. 2.0).

No overt frequency components were observed in the baseline data for the non-disabled volunteer nor during periods of muscle inactivity. However, there was a strong component during muscle activity. We did not simulate EMG during locomotion. To design a simulation that mimics the complex bursting patterns seen during stepping would be extremely difficult. The resulting SNRs from our analyses of the non-disabled subject (Figure 1) empirically suggest that our model is correctly identifying the activation patterns and there is no compelling reason why the above results do not apply to EMG during locomotion.

This limited simulation study suggests that our model is robust against departures from our assumption that between change-points the data are iid Normal and that the baseline data are iid Normal.

6. DISCUSSION

We have shown how RJMCMC simulation can be used to model the variance function of a zero-mean, heteroscedastic process and have applied our method to the analysis of EMG data. The major advantage of our method over those to date is that we can easily assess the variability of the activation patterns and, thus, of those quantities that can be computed as functions of these activation patterns. These physiological quantities, such as coactivity, can be used to diagnose pathological disorders and assess interventions.

We have used a step function to estimate the variance function, f, in equation 1. One could alternatively use a higher order spline which would result in a smoother estimate of the variance function. However, co-location of several knots may be required to model the non-smooth, either undifferentiable or discontinuous, changes in the variance function that occur at abrupt interfaces between periods of activity and inactivity. Using a step function adequately captures the salient aspects of the quantities of interest without introducing further complexities into the RJMCMC sampler. Our model also assumes normal errors. If this is inappropriate, one may use a Student's t distribution for the error terms. One must then select an appropriate choice for the number of degrees of freedom. A single choice for all inter-change-point distributions may not be appropriate and so one should include $K + 1$ extra parameters to the model with k change-points—one for each extra degree of freedom required to model the $K + 1$ inter-change-points T distributions.

We have adopted the philosophy of Loeb and Gans (1986) that in analyzing EMG signals one must consider the unique characteristics of the EMG signal in choosing a particular technique. The patterns and timing of muscle activity and inactivity are the characteristics in which we are interested. Although the data from our applications violates a model assumption, our simulation study suggests that this violation is inconsequential in light of the fact that we are not interested in estimating the frequency components within the signal.

However, if one were interested in estimating the frequency components a suggestive model might be

$$y_t = \sum_{i=1}^{K} A_{k,t} \cos(2\pi f_{k,t} t + \phi_{k,t}) + \varepsilon_t.$$

One could then use a reversible jump algorithm allowing K to vary while modeling each amplitude with a spline function. Given K, one would use a reversible jump algorithm to select the knots for each of the K spline functions. One could then define onset of muscle activity in terms of relative amplitudes of the signal and baseline data. Usually one would assume the error terms are iid. However, here one must also consider heteroscedasticity. During forceful contractions of the muscle, not only do the amplitudes and frequencies in the signal change, the associated errors increase. Thus, it is also necessary to model the heteroscedasticity—perhaps as a function of amplitude. In the Bayesian framework a second, nested, RJMCMC algorithm would then be required to model the variance function with splines or step functions.

REFERENCES

ASHBY, P. AND MCCREA, D. A. (1987). Neurophysiology of spinal plasticity. In Davidoff, R. A. (ed.), *Handbook of the Spinal Cord*, New York: Dekkar, pp. 119–143.

BERES, J. A., JOHNSON, T. D. AND HARKEMA, S. J. (2002). Clonus after human spinal cord injury cannot be attributed solely to recurrent muscle-tendon stretch. *Experimental Brain Research* (Submitted).

(1993). In Berne, R. M. and Levy, M. N. (eds), *Physiology*, 3rd edition. St. Louis, MO: Mosby Year Book.

BOLLERSLEV, T. (1986). Generalized autoregressive conditional heteroskedasticity. *Journal of Econometrics* **31**, 307–327.

BOLLERSLEV, T., CHOU, R. Y. AND KRONER, K. F. (1992). ARCH modeling in finance. *Journal of Econometrics* **52**, 5–59.

BROOKS, S. P. AND GIUDICI, P. (1998). *Convergence assessment for reversible jump MCMC simulations*, Technical Report. UK: University of Bristol.

DE BOOR, C. (1978). *A Practical Guide to Splines*. New York: Springer.

ENGLE, R. F. (1982). Autoregressive conditional heteroscedasticity with estimates of the variance of United Kingdom inflation. *Econometrica* **50**, 987–1007.

EUBANK, R. L. (1988). *Nonparametric Regression and Spline Smoothing*. New York: Marcel Dekker.

GELMAN, A. AND RUBIN, D. B. (1992). Inference from iterative simulation using multiple sequences. *Statistical Science* **7**, 457–511.

GREEN, P. J. (1995). Reversible jump Markov chain Monte Carlo computation and Bayesian model determination. *Biometrika* **82**, 711–732.

HASTINGS, W. K. (1970). Monte Carlo sampling methods using Markov chains and their applications. *Biometrika* **57**, 97–109.

HODGES, P. W. AND BUI, B. H. (1996). A comparison of computer-based methods for the determination of onset of muscle contraction using electromyography. *Electroencephalography and Clinical Neurophysiology* **101**, 511–519.

LOEB, G. E. AND GANS, C. (1986). *Electromyography for Experimentalists*. Chicago: The University of Chicago Press.

MAUGER, D. T. AND BROWN, M. B. (1995). A comparison of methods that characterize pulses in a time series. *Statistics in Medicine* **14**, 311–325.

METROPOLIS, N. *et al.* (1953). Equations of state calculations by fast computing machines. *J. Chem. Phys.* **21**, 1087–1091.

NEPTUNE, R. R., KAUTZ, S. A. AND HULL, M. L. (1997). The effect of pedaling rate on coordination in cycling. *Journal of Biomechanics* **30**, 1051–1058.

PERRY, J. (1992). *Gait Analysis: Normal and Pathological Function*. Thorofare, NJ: SLACK.

PRATT, W. K. (1991). *Digital Image Processing*, 2nd edition. New York: Wiley.

STAUDE, G. AND WOLF, W. (1999). Objective motor response onset detection in surface myoelectric signals. *Medical Engineering & Physics* **21**, 449–467.

WAHBA, G. (1990). *Spline Models for Observational Data*. Philadelphia, PA: Society for Industrial and Applied Mathematics.